Quantifying the entry efficacy among NPC1 SNP mutations reduced binding to GP of filovirus

Kwang Su Kim[1], Tatsunari Kondoh[2,], Yusuke Asai[3], Ayato Takada[2], Shingo Iwami[1,4,5,6]

[1]Department of Biology, Kyushu University, Fukuoka 8128581, Japan.

[2]Research Center for Zoonosis Control, Hokkaido University, Sapporo 0010020, Japan.

[3]Disease Control and Prevention Center, National Center for Global Health and Medicine, To kyo 1628655, Japan.

[4]MIRAI, Japan Science and Technology Agency, Saitama 3320012, Japan.

[5]CREST, Japan Science and Technology Agency, Saitama 3320012, Japan.

[6]Science Groove Inc., Fukuoka 810-0041, Japan.

1 Introduction

Filovirus particles are entered into host cells through micropinocytosis by attaching receptor C-type lectins. The glycoprotein (GP), which is the viral surface protein of filoviruses, is cleaved by the proteases cathepsin B and cathepsin L and changes to digested GP (Lee and Saphire, 2009). NPC-1 molecules located in the lysosomal membrane function as true receptors, leading to membrane fusion and entry (Simmons, 2013). NPC1 is essential host factor and important for ebolavirus replication (Herbert et al., 2015; Li et al., 2016).

Recently, Wang et al. showed that amino acid substitution in the two loops on NPC1, which is presented in the structure of ebola digested glycoprotein (dGP), reduces the binding to dGP (Wang et al., 2016). To identify the influence of single-nucleotide polymorphisms (SNPs) on host susceptibility to filovirus infection, Kondoh et al. investigated cell susceptibility for 10 missense SNPs in the GP-interacting loop regions of NPC (Kondoh et al., 2018). They found that P424A & D508N and S425L & D502E substitutions in NPC1 reduced the entry of VSVΔG-EBOV and VSVΔG-MARV, respectively. These findings suggest that different SNPs affect virus entry process and it cause different entry efficacy in **Figure 1A**.

However, during plaque forming, these results derived by complex process including cell-cell infection, viral productional time, latent time, intracellular replication. It is difficult to convert the multi-composed kinetics of viral infection into parameters from this complexity process, but mathematical modeling and numerical simulation methods of experimental data

enable this (Iwami et al., 2012; Iwanami et al., 2017). In particular, purpose of this study is to quantitatively analyze how some SNPs more effectively affect the virus entry through mathematical modeling. Toward this goal, we performed two experiments. Firstly, NPC1-knockout Vero E6 cell lines and established stable cell lines expressing the NPC1 SNP mutants. To compare the virus infectivity, we performed a plaque assay on 5 types SNP mutations with 2NPC1 for VSVΔG-EBOV and VSVΔG-MARV, respectively (see **Figure 1 B**).

In this study, we suggest mathematical model to describe virus amplification in the plaque with considering virus producing period. Numerical solution of mathematical model can describe a plaque expantion and merging process that is similar to the actual phenomenon occurring in the plate. Our suggested mathematical model can fit time-course of plaque size data and obtain quantitative entry efficacy values for each SNP mutations.

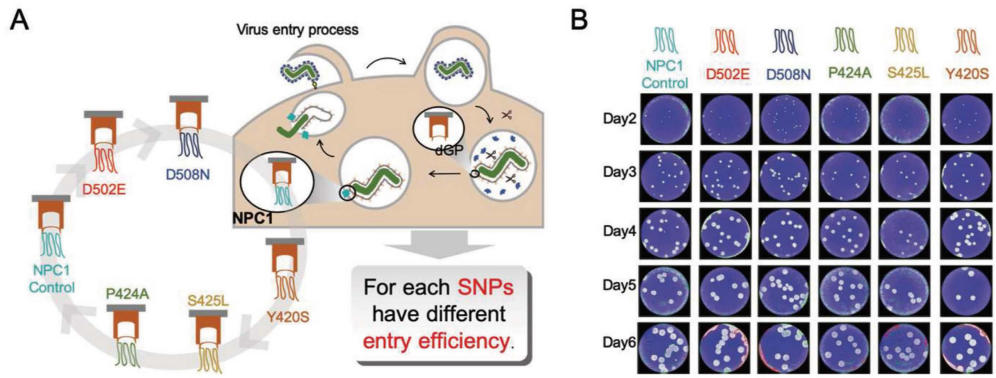

Figure 1. A. Ebola virus entry efficiency is different depend on SNPs. **B.** plaque assay time course of data sets depend on SNPs

2 Mathematical model considering virus dynamics to analyze plaque assay data

Before construct mathematical model, we know that radius of plate is 17.35mm and average of cell radius is 0.004mm as we measured. Since interval of between cell is 0.008mm, we can assume that there is $\frac{17.35mm}{0.008mm} = 2169$ circle line where cell is distributed in the plate. If the circumference of the circle line is divided by the diameter of the cell, the number of cells distributed in one circle line can be obtained, which is proportional to the diameter of the circle line.

After considering cell number and circle line, we suggest the following basic mathematical model which represent the dynamics of virus infection depend on time (t) and radius (r):

$$\begin{aligned}
\frac{dT(t,r)}{dt} &= -\omega T(t,r)I(t,r-\Delta r),\\
\frac{dE(t,r)}{dt} &= \omega T(t,r)I(t,r-\Delta r) - kE(t,r),\\
\frac{dI(t,r)}{dt} &= kE(t,r) - \delta I(t,r),\\
\frac{dD(t,r)}{dt} &= \delta I(t,r),
\end{aligned} \tag{1}$$

with initial condition:

$I = \begin{cases} \frac{2\pi\times r}{0.008}, & r \le r_0 \\ 0, & r > r_0 \end{cases}$ at $t = 0$, $T = \begin{cases} 0, & r \le r_0 \\ \frac{2\pi\times r}{0.008}, & r > r_0 \end{cases}$ at $t = 0$, and $E, D =$ 0 at $t = 0$ for all values of r.

T, E, I and D is the number of target cell, eclipse phase cell, infectious cell (virus producing cell) and dead cell. We just consider cell-cell infection in model (1), because agar used in our experiment limit the virus-transmission. It was assumed that there is no cell growth, only the infected cells injected at the initial stage were distributed below the radius r_0, and that the target cells were not present in the this interval and were linearly increasingly distributed depend on radius of circle line in the circle line exceeding r_0. Since the infection spreads from a small circle to a large one, the target cell located at specific radius (r^*) is infected by infected cells located in ($r^* - \Delta r$) directly inside at an infection rate of ω where Δr is interval (0.008mm) of circle line. After target cell infected by infected cell became eclipse phase cell, they exponentially changes from eclipse phase to infectious cell phase at rate k as time goes on. Infectious cell become dead cell at a rate δ(see **Figure 2**).

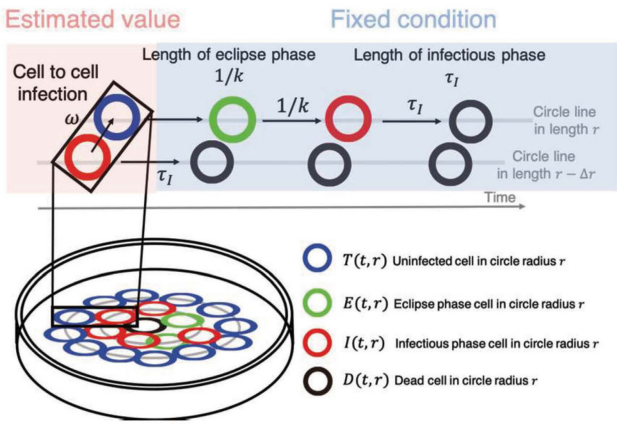

Figure 2. Schematic diagram of virus dynamics in model (1) for descrb ing plaque amplification.

3 Data fitting

For describing amplification of plaque, the our base model (1) has 4 parameters: initial radius of infectious cell area (r_0), infection rate (ω), the changing rate from exposed stage cell to

infectious state (k) and the death rate of virus-producing cells (δ). Firstly, we estimated and fixed parameter about eclipse cell and infectious phase cell from data of measuring infectious phase and eclipse phase. In experiments, each area of plaques are obtained for each measurement day. Then, we can calculate radius of plaque from area from day2 to day6 (see **Figure 3 A**). To estimate infection rate (ω) and initial radius of infectious cell (r_0), we used the plaque radius of each day, and because the measured plaque number and radius of each plaque were different (see **Figure 3 B**). We used the weighted lease square method considering the mean and standard deviation of the observations. The sum of the residuals depend on infection rate and initial radius of infectious cell, $SSR(\omega, r_0)$, is defined as

$$SSR(\omega, r_0) = \sum_{i=2}^{6} \frac{1}{sd_i^2} \left(D_i - M_i(\omega, r_0)\right)^2$$

where D_i, sd_i and M_i are the mean, standard deviation of plaque radius data and model result, for each day $i = 2,3,\ldots,6$, respectively.

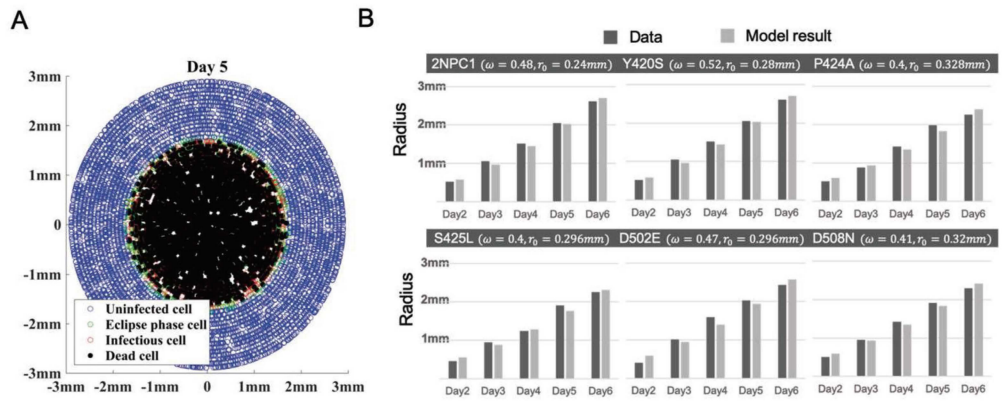

Figure 3. A Simulated model results for model (1) at day 5. **B** Data fitting results and estimated parameters depend on SNPs.

4 Discussion

Adding biologically realistic complexity to a model does not necessarily improve the ability of the model to describe the experimental data set. Previous models which described the plaque expansion considered the diffusion of virus (Alvarez et al., 2007; Haseltine et al., 2008), but under our experimental conditions, the cells were fixed with agar and only cell-cell infection occurred. The ODE model, which depends on mass action kinetics, assumes that all infectious cells can contribute to cell-to-cell infection (Kumberger et al., 2018). However, in the case of fixed cells, the proportion of infectious cells varies with increasing focus. For example, the inside of the plaque is dead cell, which is infectious and only the target cell that is adjacent to the infectious cell is possible. To represent this, our model consider only the infection of the of

the neighboring cells in the circle line considering the cell spacing located on the plate, not considering the diffusion of the virus.

Summarizing, our results using plaque assay and directly measurement of virus producing time focus on differences of entry efficacy among SNP mutations. In this investigation, our modeling approach can allow us to describe plaque amplification, merging of plaque and fit plaque radius data. Throughout this process, SNPs amino acid mutation's entry efficacy was quantified and sequenced. These results help us to understand the susceptibility of humans genetic polymorphism to filoviruses. There is abundant space for further progress in analyzing the effect of different entry among SNPs by combining experiments and mathematical modeling.

References

[1] Lee, J. E., Saphire, E. O., 2009. Ebolavirus glycoprotein structure and mechanism of entry. Future Virology 4, 621-635.

[2] Simmons, G., 2013. Filovirus Entry. Viral Entry into Host Cells 790, 83-94.

[3] Wang, H., Shi, Y., Song, J., Qi, J. X., Lu, G. W., Yan, J. H., Gao, G. F., 2016. Ebola Viral Glycoprotein Bound to Its Endosomal Receptor Niemann-Pick C1. Cell 164, 258-268.

[4] Kondoh, T., Letko, M., Munster, V. J., Manzoor, R., Maruyama, J., Furuyama, W., Miyamoto, H., Shigeno, A., Fujikura, D., Takadate, Y., Yoshida, R., Igarashi, M., Feldmann, H., Marzi, A., Takada, A., 2018. Single-Nucleotide Polymorphisms in Human NPC1 Influence Filovirus Entry Into Cells. Journal of Infectious Diseases 218, S397-S402.

[5] Iwami, S., Sato, K., De Boer, R. J., Aihara, K., Miura, T., Koyanagi, Y., 2012. Identifying viral parameters from in vitro cell cultures. Frontiers in Microbiology 3.

[6] Iwanami, S., Kakizoe, Y., Morita, S., Miura, T., Nakaoka, S., Iwami, S., 2017. A highly pathogenic simian/human immunodeficiency virus effectively produces infectious virions compared with a less pathogenic virus in cell culture. Theoretical Biology and Medical Modelling 14.

[7] Alvarez, L. J., Thomen, P., Makushok, T., Chatenay, D., 2007. Propagation of fluorescent viruses in growing plaques. Biotechnology and Bioengineering 96, 615-621.

[8] Haseltine, E. L., Lam, V., Yin, J., Rawlings, J. B., 2008. Image-guided modeling of virus growth and spread. Bulletin of Mathematical Biology 70, 1730-1748.

[9] Kumberger, P., Durso-Cain, K., Uprichard, S. L., Dahari, H., Graw, F., 2018. Accounting for Space - Quantification of Cell-To-Cell Transmission Kinetics Using Virus Dynamics Models. Viruses 10, 2000.

Research Institute for Mathematical Sciences

Kyoto University

Kyoto 606-8502

JAPAN

E-mail address: kwangsu815@gmail.com